Electronic Supplementary Material

Optimizing iodine capture performance by metal-organic framework containing with bipyridine units

Xinyi Yang[1,2], Xiaolu Liu[2], Yanfang Liu[2], Xiao-Feng Wang (✉)[1], Zhongshan Chen[2], Xiangke Wang (✉)[2]

1 School of Chemistry and Chemical Engineering, University of South China, Hengyang 421001, China

2 College of Environmental Science and Engineering, North China Electric Power University, Beijing 102206, China

E-mails: xfwang518@sina.cn (Wang X-F); xkwang@ncepu.edu.cn (Wang X)

Chemicals and instruments

All chemicals were sourced from commercial suppliers and used without further purification. Powder X−ray diffraction (PXRD) patterns were collected on a Rigaku SmartLab SE X−ray diffractometer equipped with a Cu Kα source. Elemental analysis data were collected on a UNICUBE elemental analyzer. BET surface areas were determined from N_2 adsorption/desorption isotherms collected at 77 K using a Micromeritics TriStar II. Scanning electron microscopy (SEM) images were recorded on a Legulus 8220 Scanning Electron Microscope. X−ray photoelectron spectroscopy (XPS) analyses were performed using a Thermo Scientific ESCALAB 250Xi spectrometer, equipped with a monochromatic Al Kα X−ray source. Fourier transform infrared spectra (FT-IR) were recorded on a SHIMADZU IRTracer−100. Thermogravimetric analysis (TGA) data was obtained by heating the sample from 25 °C to 800 °C using a STA 2500 under 10K/min N_2 atmosphere. Raman spectra were collected on a high-resolution confocal Raman system (LabRam HR800, Horiba Jobin Yvon, Japan) using 514 nm lasers.

Materials characterization

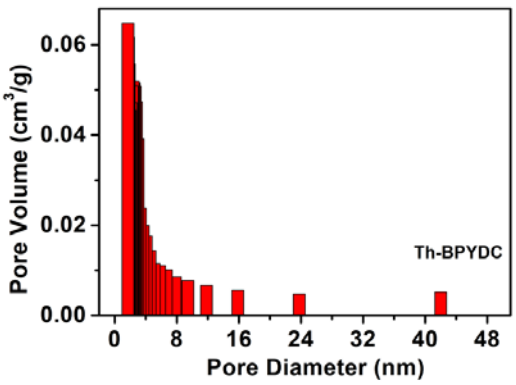

Fig. S1 Pore size distribution plot for **Th-BPYDC** from N_2 isotherms measured at 77 K.

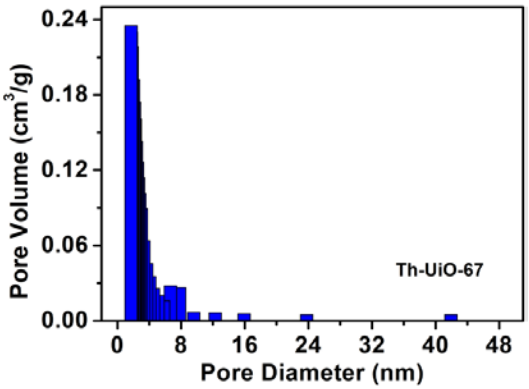

Fig. S2 Pore size distribution plot for **Th-UiO-67** from N_2 isotherms measured at 77 K.

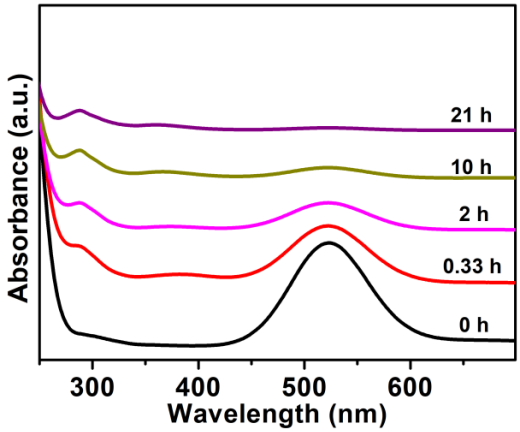

Fig. S3 UV-Vis absorption spectra of iodine solutions in the presence of **Th-BPYDC** at different time.

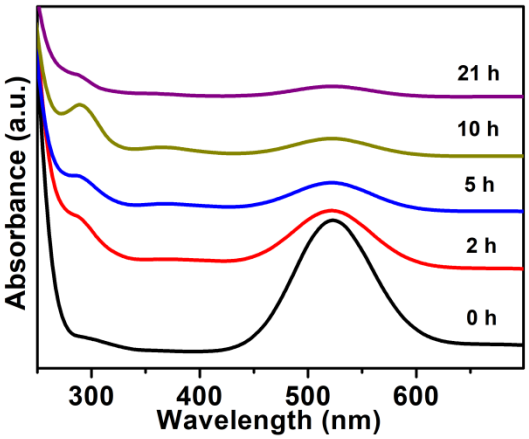

Fig. S4 UV-Vis absorption spectra of iodine solutions in the presence of **Th-UiO-67** at different time.

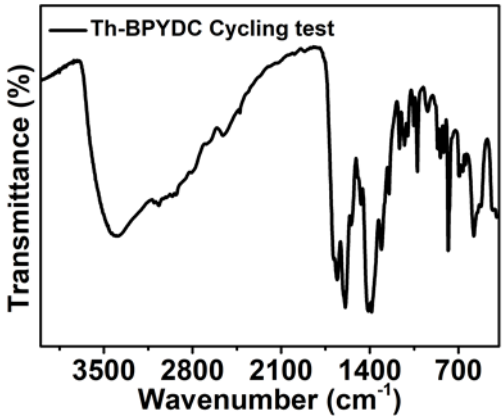

Fig. S5 FT-IR of **Th-BPYDC** after 4 cycles of iodine adsorption/release in cyclohexane.

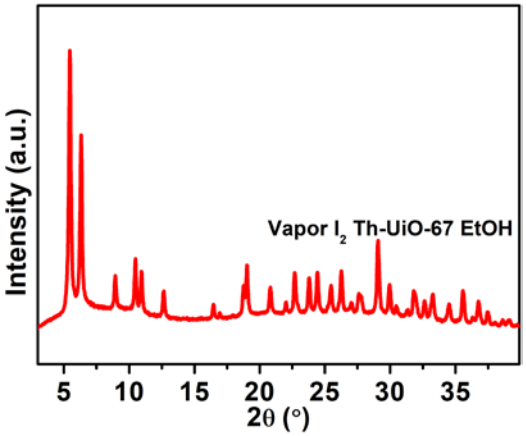

Fig. S6 PXRD of **Th-UiO-67** after iodine vapor release in ethanol.

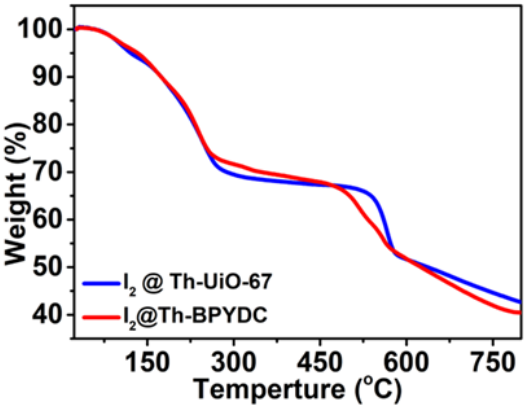

Fig. S7 TGA diagrams of **Th-BPYDC** and **Th-UiO-67** after adsorption of iodine in cyclohexane solution.

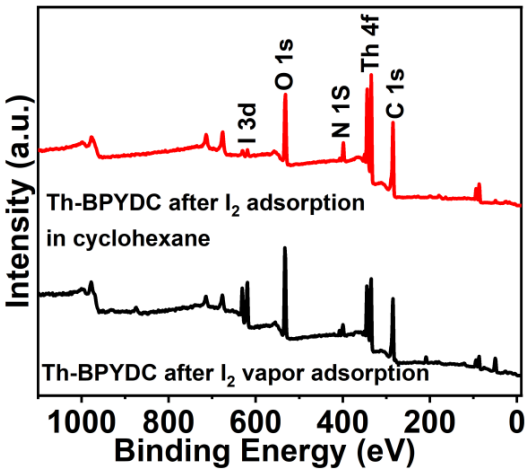

Fig. S8 Full survey XPS spectra of **Th-BPYDC** after adsorption of iodine.

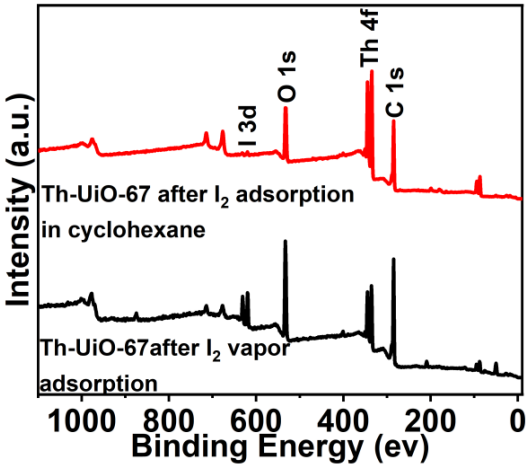

Fig. S9 Full survey XPS spectra of **Th-UiO-67** after adsorption of iodine.

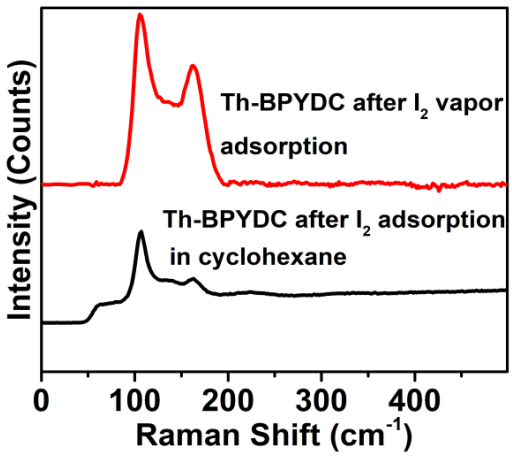

Fig. S10 The Raman spectra for **Th-BPYDC** after iodine adsorption.

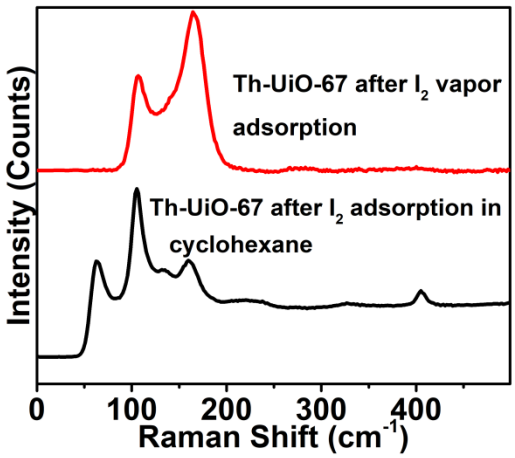

Fig. S11 The Raman spectra for **Th-UiO-67** after iodine adsorption.

Table S1. Elemental analysis of **Th-UiO-67** and **Th-BPYDC**.

Materials	Element content		
	C(%)	N(%)	H(%)
Th-UiO-67	30.34	1.01	2.365
Th-BPYDC	31.60	9.35	3.900

Table S2. Langmuir and Freundlich adsorption parameters for iodine adsorption on different adsorbents in cyclohexane.

Materials	Langmuir isotherm			Freundlich isotherm		
	K_L	q_m (mg/g)	R^2	K_F	*1/n*	R^2
Th-UiO-67	0.2821	229.3	0.9626	78.61	0.1618	0.9343
Th-BPYDC	0.3196	481.2	0.9853	125.4	0.1524	0.9577

Table S3. Summary of adsorption kinetic parameters for iodine adsorption on different adsorbents in cyclohexane.

Materials	$q_{e,exp}$ (mg/g)	Pseudo−first−order model			Pseudo−second−order model		
		$q_{1,cal}$ (mg/g)	K_1 (min^{-1})	R^2	$q_{2,cal}$ (mg/g)	K_2 (mg/g/min)	R^2
Th-UiO-67	93.84	91.1534	0.4306	0.9980	102.52	0.00578	0.9983
Th-BPYDC	98.53	87.76	1.7041	0.9477	98.80	0.02239	0.9912